Feeding and energetics of the great scallop, Pecten maximus, through a DEB model

Romain Lavaud, Jonathan Flye-Sainte-Marie, Fred Jean, Antoine Emmery,
Oivind Strand, Sebastian, A.L.M. Kooijman

▶ **To cite this version:**

HAL Id: hal-00917710

https://hal.univ-brest.fr/hal-00917710

Submitted on 13 Dec 2013

Feeding and energetics of the great scallop, *Pecten maximus*, through a DEB model

Romain Lavaud[a,*], Jonathan Flye-Sainte-Marie[a], Fred Jean[a], Antoine Emmery[b], Øivind Strand[c], Sebastiaan A.L.M. Kooijman[d]

[a]*Laboratoire des sciences de l'environnement marin (UMR6539 CNRS/IRD/UBO), Institut Universitaire Européen de la Mer, Université de Brest, Plouzané, France*
[b]*Station expérimentale d'Argenton (Ifremer), Argenton, France*
[c]*Institute of Marine Research (IMR), Bergen, Norway*
[d]*Department of Theoretical Biology, Institute of Ecological Science, Vrije Universiteit, Amsterdam, The Netherlands*

Abstract

We developed a full life-cycle bioenergetic model for the great scallop *P. maximus* relying on the concepts of the Dynamic Energy Budget (DEB) theory. The covariation method was implemented to estimate the parameters of a standard DEB model. Such models are able to predict various metabolic processes from a food availability marker and temperature in the environment. However, suspension-feeders are likely to feed on various trophic sources, from microalgae cells to detritus. They are also able to sort and select food particles very efficiently, depending on their size, energetic value or quality. The present model includes a mechanistic description of the feeding processes, based on Kooijman's Synthesizing Unit principle which allow to deal with several food sources. Moreover we tested the hypothesis of a differential selectivity between two potential substrates (phytoplankton cell and the remaining particulate organic matter). Simulations of shell length, daily shell growth rate, dry weight and gonado-somatic index (GSI) variations were realized and compared to field data from a monitoring conducted in the Bay of Brest (Brittany, France) for six years. The model shown its capacity to efficiently reproduce all life history traits of the wild great scallops. Predicted length data were estimated to the nearest millimeter. The fit of simulated weights to observed data was very satisfactory. GSI predictions were also in accordance with observations but improvements are required to better capture the sharp increase of gametogenesis at the beginning of the year. Finally, results bring evidences that *P. maximus* is actually preferentially feeding on living algae cells rather than on the rest of organic particles.

Keywords: Pecten maximus, DEB theory, Synthesizing Units, Phytoplankton, Feeding process, Bay of Brest

∗. Corresponding author. Tel.: +33 2 98 49 86 70; Fax: +33 2 98 49 86 45
  Email addresses: romain.lavaud@univ-brest.fr (Romain Lavaud), romain.lavaud@hotmail.fr (Romain Lavaud)

1. Introduction

The great scallop *Pecten maximus* (Linnaeus, 1758) is a bivalve mollusk living in coastal environments of North-Western Atlantic, commercially important for fisheries and sea ranching. A large number of studies has long explored the physiological and ecological traits of this animal, both in controlled environment and in the wild (e.g. Mason, 1957; Antoine et al., 1979; Paulet et al., 1997; Saout et al., 1999; Laing, 2000; Chauvaud et al., 2001; Laing, 2002; Strohmeier et al., 2009; Chauvaud et al., 2012). Its broad latitudinal and bathymetric distribution results in a variability of life history traits with a large ultimate size in Northern environments and small size in Southern areas and deep locations (Chauvaud et al., 2012). Known to feed mainly on phytoplankton and microphytobenthos (Robert et al., 1994; Chauvaud et al., 2001), its diet has also been reported to include bacteria and nanoplankton as well (Heral, 1989; Langdon and Newell, 1990; MacDonald et al., 2006; Nerot et al., 2012), but in proportion that still need to be assessed. These two aspects of *P. maximus* biology (growth and feeding) are key processes for a better comprehension of the physiology of this species.

Within the French project COMANCHE, we are trying to combine various scientific and economic approaches around the biology and exploitation of *P. maximus* in the English Channel region. The development of a bioenergetic individual-based model is a crucial step to combine hydrodynamic, larval development and dispersion models with population dynamic modeling. Thus we were motivated to set up a mechanistic model capable, with as few variables as possible, to simulate the evolution through time of diverse physiological traits that would serve as basis for fishery management.

We tried to combine knowledge accumulated about this species in a model for metabolic processes, which can give reliable insights on the physiological evolution of the organism and thus capture the variability observed in biological pattern. Dynamic Energy Budget theory (DEB, Kooijman, 2010) provides such a generalized, individual-based, bioenergetic framework suitable for linking levels of metabolic organization through a mechanistic model. It has been successfully applied to 240 species from fungi to mammals (Kooijman, 2013) and especially to bivalves species closely related to *P. maximus* such as *Crassostrea gigas* in the same taxonomic order (Pouvreau et al., 2006; Cardoso et al., 2006; Bourlès et al., 2009; Alunno-Bruscia et al., 2011; Bernard et al., 2011), *Mytilus edulis* (Cardoso et al., 2006; Rosland et al., 2009; Troost et al., 2010; Saraiva et al., 2011a), *Ruditapes philippinarum* (Flye-Sainte-Marie et al., 2007), *Perna canaliculus* (Ren and Ross, 2005), *Cerastoderma edule* (Cardoso et al., 2006; Troost et al., 2010; Wijsman and Smaal, 2013), *Macoma baltica*, *Mya arenaria* (Freitas et al., 2009) and *Pinctada margaritifera* (on the larval stage Thomas et al., 2011).

In this study we aim at developing the first DEB model for a member of the pectinid family, *P. maximus*. Using literature data we estimated the standard DEB parameters and built our model with the Synthesizing Units concept

(Kooijman, 2010). The inter-annual variability of several physiological processes of adult scallops was studied and compared to monitoring data gathered over six years in the Bay of Brest (Brittany, France). An innovative aspect of this work is the implementation of the hypothesis of a differential selectivity in food sources, tested using the Synthesizing Units principle from Kooijman (2010).

2. Material and methods

2.1. Model formulation

The model developed in this study is based on the Dynamic Energy Budget theory (Kooijman, 2010). According to DEB theory the energetics of an organism can be described by the dynamics of three state variables: (1) the structural volume V (somatic tissue excluding reserves), (2) the reserves E and (3) the energy allocated to maturity and reproduction E_R. Trophic resource provides energy that fuels the reserve compartment. A fixed fraction (κ) of energy flux from reserve is then allocated to somatic growth plus its maintenance, with a priority given to maintenance. The remaining fraction ($1 - \kappa$) is used for maturity maintenance, maturation (in embryos and juveniles) and reproduction (i.e. gamete production in adults). A conceptual scheme, illustrating the modeled energy flows through the scallop, is given in Fig. 1. Notation of the variables and parameters is from Kooijman (2010).

In this study, we paid a particular attention to the feeding process, which is rather complex in suspension feeders (Ward and Shumway, 2004; Cranford et al., 2011). Briefly, the filtering process in bivalves can be described as follows. A water current is generated through the pallial cavity by ciliary activity of the gills. Water is then sieved by the gills, the amount of water totally cleared of its particles per unit of time is denoted as clearance (or filtration) rate $\dot{F}_X$. For each food particle present in the surrounding water, with a density X, the flux of particles extracted from the environment, known as consumption rate, can be assessed by $X\dot{F}_X$. Rubbed into mucus strings, food particles are then transported to the aboral side of the gills where labial palps sort and bring food pellets to the mouth for ingestion ; this ingestion rate is denoted as $\dot{J}_{Xm}$. Suspension feeding bivalves are known to feed upon various trophic sources (see e.g. Kamermans, 1994; Chauvaud et al., 2001; MacDonald et al., 2006; Bachok et al., 2009; Yokoyama et al., 2009; Nerot et al., 2012) and they are subsequently able to develop a plastic trophic niche, variable in space and time as an adaptation/acclimation to available trophic resources and depending on their development stage (Rossi et al., 2004; Marín Leal et al., 2008). Filtration, ingestion and assimilation processes are characterized by a capacity to select and sort potential food particles, via gill crossing retention, labial palps selectivity, inner digestive gland sorting, differential assimilation rates. Moreover, many studies focusing on modelling the energy dynamics of filter feeders have reported the need (Alunno-Bruscia et al., 2011; Bernard et al., 2011) and the benefit (Troost et al., 2010; Saraiva et al., 2011b) of adding a second food source to forcing variables to improve the food proxy . Thus, to model energy

3

acquisition and afterwards its dynamics in *P. maximus* we focused on two concepts: (1) the processing of two types of

food substrates and (2) the selectivity of food particles of different origins and energetic values.

In order to address these issues we chose to work with the concept of Synthetizing Units (SUs, Kooijman, 1998,

2006, 2010; Saraiva et al., 2011b), considered as generalized enzymes that transform an arrival flux of substrates into

a production flux of products. Here food particles are considered as substrates and reserves as products. During the

processing (handling time), no substrate particles are accepted by the SU, i.e. while handling, the binding probability

for each arriving substrate will be null. SUs allow to deal with different types of food to test some patterns in feeding

such as selectivity of substrates. We used two potential trophic sources markers: algal cell counting and the rest of

particulate organic matter (POM, i.e. non algal organic particles). Substrates were respectively called S_X for cell

counting and S_Y for POM. The arrival flux of food particles was taken to be proportional to the density in spatially

homogeneous environments (Kooijman, 2010), which is the case in aquatic environments. We worked with interacting

substitutable substrates that are bound in a sequential fashion (Fig. 2). This scheme illustrate the possibility for a free

SU ($\theta.$) to bind to either a substrate particle from type S_X or S_Y to form a SU-S_X complex (θ_X) or a SU-S_Y complex

(θ_X) respectively. Moreover, a substrate S_X can replace a S_Y in a SU-S_Y complex (θ_Y) to form a SU-S_X complex

(θ_X), releasing an untransformed substrate S_Y. Each food type contributes to the production of reserves, specified in

yield coefficients (y_{EX} and y_{EY}) that were here treated as constant. Given the dissociation rate parameters $\dot{k}_X$ and

$\dot{k}_Y$, the binding parameters $\dot{b}_X$ and $\dot{b}_Y$ and the interaction affinities $\dot{b}_{XY}$ and $\dot{b}_{YX}$, the change in binding fractions for

substrates X and Y are:

$$\frac{d}{dt}\theta. = \dot{k}_X\theta_X + \dot{k}_Y\theta_Y - (\dot{b}_X X + \dot{b}_Y Y)\theta. \tag{1a}$$

$$\frac{d}{dt}\theta_X = -\dot{k}_X\theta_X + \dot{b}_X X\theta. - \dot{b}_{YX}Y\theta_X + \dot{b}_{XY}X\theta_Y \tag{1b}$$

$$\frac{d}{dt}\theta_X = -\dot{k}_X\theta_X + \dot{b}_X X\theta. - \dot{b}_{YX}Y\theta_X + \dot{b}_{XY}X\theta_Y \tag{1c}$$

$$\frac{d}{dt}\theta_Y = -\dot{k}_Y\theta_Y + \dot{b}_Y Y\theta. + \dot{b}_{YX}Y\theta_X - \dot{b}_{XY}X\theta_Y \tag{1d}$$

with $1 = \theta. + \theta_X + \theta_Y$ and X and Y stand for the densities of substrates S_X and S_Y in a number of particle per liter.

The pseudo steady state fractions are:

$$\theta_X^* = \frac{\alpha_Y\dot{b}_X X - \beta_X\dot{b}_Y Y}{\alpha_X\alpha_Y - \beta_X\beta_Y}; \qquad \theta_Y^* = \frac{\alpha_X\dot{b}_Y Y - \beta_Y\dot{b}_X X}{\alpha_X\alpha_Y - \beta_X\beta_Y} \tag{2}$$

with

$$\alpha_X = \dot{k}_X + \dot{b}_X X + \dot{b}_{YX} Y; \qquad\qquad \alpha_Y = \dot{k}_Y + \dot{b}_Y Y + \dot{b}_{XY} X; \tag{3a}$$

$$\beta_X = \dot{b}_X X - \dot{b}_{XY} X; \qquad\qquad \beta_Y = \dot{b}_Y Y - \dot{b}_{YX} Y \tag{3b}$$

The preference hypothesis is transcribed into the model by changing $\dot{b}_{XY}$ and $\dot{b}_{YX}$, in such a way that the SU would be able to change from substrate X to substrate Y, i.e. setting one probability superior to the other. $\dot{b}_{XY}$ and $\dot{b}_{YX}$ were first turned into $\{\dot{b}_{XY}\} = \dfrac{\dot{b}_{XY}}{L^2}$ and $\{\dot{b}_{YX}\} = \dfrac{\dot{b}_{YX}}{L^2}$, to get rid of size dependency. $\{\dot{b}_{YX}\}$ was set at 0 and $\{\dot{b}_{XY}\}$ was taken equal to the maximum specific filtration rate for X-type substrate, $\{\dot{F}_{Xm}\}$. In this case a change in the substrate to process may occur in one direction only. When both substrates are available, this rule leads to an automatic substitution of the counter-selected substrate (POM particle), already bound to a SU, by the preferred food type (here algae cells). Dissociation rates relate to the maximum specific feeding rates as $\dot{k}_X = \{\dot{h}_{XAm}\} L^2$ and $\dot{k}_Y = \{\dot{h}_{YAm}\} L^2$, where L is the structural length of the individual and $\{\dot{h}_{XAm}\}$ and $\{\dot{h}_{YAm}\}$ are the maximum specific feeding rates ($\#.\mathrm{d}^{-1}.\mathrm{cm}^{-2}$), given by:

$$\{\dot{h}_{XAm}\} = \frac{\{\dot{J}_{XAm}\}}{M_X} \quad \text{with} \quad \{\dot{J}_{XAm}\} = \frac{\{\dot{p}_{Am}\}}{(\mu_E \, y_{EX})} \tag{4a}$$

$$\{\dot{h}_{YAm}\} = \frac{\{\dot{J}_{YAm}\}}{M_Y} \quad \text{with} \quad \{\dot{J}_{YAm}\} = \frac{\{\dot{p}_{Am}\}}{(\mu_E \, y_{EY})} \tag{4b}$$

where $\{\dot{J}_{XAm}\}$ and $\{\dot{J}_{YAm}\}$ are the maximum specific ingestion rates ($\mathrm{mol.d}^{-1}.\mathrm{cm}^{-2}$), $\{\dot{p}_{Am}\}$ is the maximum specific assimilation rate ($\mathrm{J.d}^{-1}.\mathrm{cm}^{-2}$), μ_E is the chemical potential of reserve ($\mathrm{J.mol}^{-1}$) and y_{EX} and y_{EY} are the yields of reserve on compound X and Y respectively ($\mathrm{mol.mol}^{-1}$). Values for these parameters are given in Table 3.

Finally, the association rates relate to the maximum specific searching rates as $\dot{b}_X = \{\dot{F}_{Xm}\} L^2$ and $\dot{b}_Y = \{\dot{F}_{Ym}\} L^2$. Thus the specific assimilation rate for reserve can be written as:

$$\dot{J}_{EA} = y_{EX} \{\dot{J}_{XAm}\} f_X + y_{EY} \{\dot{J}_{YAm}\} f_Y \tag{5}$$

with

$$f_X = \frac{\alpha_Y \{\dot{F}_{Xm}\} X - \beta_X \dot{b}_Y Y}{\alpha_X \alpha_Y - \beta_X \beta_Y}; \qquad\qquad f_Y = \frac{\alpha_X \{\dot{F}_{Ym}\} Y - \beta_Y \dot{b}_X X}{\alpha_X \alpha_Y - \beta_X \beta_Y} \tag{6a}$$

$$\alpha_X = \{\dot{h}_{XAm}\} + \{\dot{F}_{Xm}\} X + \{\dot{b}_{YX}\} Y; \qquad \alpha_Y = \{\dot{h}_{YAm}\} + \{\dot{F}_{Ym}\} Y + \{\dot{b}_{XY}\} X \tag{6b}$$

$$\beta_X = \{\dot{F}_{Xm}\} X - \{\dot{b}_{XY}\} X; \qquad\qquad \beta_Y = \{\dot{F}_{Ym}\} Y - \{\dot{b}_{YX}\} Y \tag{6c}$$

In order to test the hypothesis of a selectivity in feeding in *P. maximus*, a classical functional response was also calculated, using only one food source (phytoplankton cells). This response to food density variations is based on the

Holling type II functional response (Kooijman, 2010) : $f = \dfrac{X}{X + X_K}$, with X the algae cell concentration (#.L^{-1}) and X_K the half-saturation coefficient (#.L^{-1}). The value of this parameter was calibrated for each year.

Once assimilation has been implemented, reserves dynamics can be treated. Energy conservation law implies that reserves dynamics amounts to the difference between the assimilation rate $\dot{p}_A$ and the utilization rate of reserves $\dot{p}_C$. The structural growth is provided with a fraction κ of this mobilized energy from which somatic maintenance requirements are first paid. The rest of energy flux from the reserve compound is allocated in priority to maturity maintenance and then to the reproduction buffer E_R. During periods of low food availability or prolonged starvation (especially in winter), *P. maximus* is known to undergo a sharp decrease in flesh weight (Comely, 1974; Pazos et al., 1997). In fact, the flux of energy coming from reserves is not sufficient to "pay" maintenance costs (both $\dot{p}_M$ and $\dot{p}_J$). The energy that has to be mobilized to pay somatic maintenance ($\dot{p}_{S1}$) and maturity maintenance ($\dot{p}_{S2}$) is taken from the reproduction buffer (resorption of gonad, $\dot{p}_{RS}$) and if the reproduction buffer is empty, maintenance costs are "paid" from the structural volume (lysis of structure, $\dot{p}_{VS}$).

The dependency of physiological rates on body temperature in ectothermes (in which body temperature equals external temperature) has been described by the Arrhenius relationship within a species-specific tolerance range of temperature (Kooijman, 2010). The following relationship was used to correct all model fluxes for temperature:

$$\dot{k}(T) = \dot{k}_1 T_C \quad \text{with} \quad T_C = \frac{\exp\left(\dfrac{T_A}{T_1} - \dfrac{T_A}{T}\right)\left(1 + \exp\left\{\dfrac{T_{AL}}{T_1} - \dfrac{T_{AL}}{T_L}\right\}\right)}{1 + \exp\left(\dfrac{T_{AL}}{T} - \dfrac{T_{AL}}{T_L}\right)} \tag{7}$$

where $\dot{k}(T)$ is the value of the physiological rate at temperature T, $\dot{k}_1$ is the physiological rate at the reference temperature T_1, T_A is the Arrhenius temperature, T_L is the lower boundary of the tolerance range, and T_{AL} is the Arrhenius temperature for the rate of decrease at the lower boundary. All temperatures are expressed in Kelvin (K).

2.2. Parameter estimation

The Arrhenius temperature was estimated by fitting the previous equation in a composite data set relating physiological rates (respiration, growth, filtration, assimilation) to temperature, constructed from data available in literature (Laing, 2000, 2002, 2004) and from unpublished studies in the Bay of Brest (Chauvaud and Paulet, unpublished data). A reference temperature (T_1) of 288 K was chosen. We applied the covariation method for parameter estimation according to the procedure described by Lika et al. (2011) that allow to estimate all parameters of the standard DEB model from empirical datasets of the literature (Table 4). Part of these observed data consists of single values, named zero-variate data, such as age, weight and size at the larval stage (Gruffydd and Beaumont, 1972; Buestel et al., 1982; Samain et al., 1986; Shumway and Parsons, 2006), at puberty (Shumway and Parsons, 2006) and for the adult period

(Paulet and Fifas, 1989; Paulet et al., 1997; Le Pennec et al., 2003; Shumway and Parsons, 2006). The other type of observations used for parameter calibration is a data set of 288 shell length over age values (EVECOS data base provided by "Observatoire Marin de l'IUEM, INSU, Plouzané"). The covariation method is a single-step procedure based on the simultaneous minimization of the weighted sum of squared deviations between all observation data sets and model predictions. Weight coefficients can be applied to zero-variate data, in order to quantify the certainty of life history traits gathered from literature (on the basis of their reliability and occurrence). Therefore, little less weight was given to puberty data as the timing of this maturity threshold is rather imprecise. Likewise, as ultimate length is an empirical measurement, hardly reproducible, a lower weight coefficient was also applied to this value. The relevance of the parameter set was assessed by a mean relative error calculation (mre).

2.3. Study site, forcing and calibration data

To test the estimated parameters we used a data set of a monthly monitoring of *P. maximus* bank located in the Roscanvel site, in the central area of the Bay of Brest (Fig. 3). This location is a coastal semi enclosed area located in Western France. It is under the influence of high tides and freshwater inputs from two rivers and is connected to the open ocean by a narrow strait (2 km wide). Biometry measurements of scallops from the Roscanvel bank (4°30'W, 48°20'N) has been monitored during several decades (1977 to 2004) and provides a large data set, also including environmental variables. Twenty scallops from the three-year age cohort (2.5 to 3.5 years old) have been collected twice a month (EVECOS data base provided by "Observatoire Marin de l'IUEM, INSU, Plouzané").

Dry weight of each organ, shell height and gonado-somatic index (gonad dry weight over total body dry weight) were measured on these individuals. In order to compare weight values obtained for different size animals, dry weights were corrected for size differences between individuals following the formula of Bayne et al. (1987):

$$W_r = \left(\frac{L_r}{L_m}\right)^3 W_m \tag{8}$$

where W_r is the recalculated weight of an individual of standard shell height L_r and W_m is the measured weight for an individual of measured shell height L_m. Length were estimated after measuring the mean daily shell growth rate (DSGR) over an entire growth season using the method proposed by Chauvaud et al. (2012). Each year, five individuals were sampled in December, i.e. after the growth cessation, to capture the entire growth season. Five other individuals harvested in August were used to assign calendar dates to each increment, by knowing the sampling date of the last formed increment. A synchronization procedure was used between the individual growth trajectories within each pool by minimizing the sum of the differences between individual series considered two-by-two. Growth trajectories from the summer pool and the winter pool were finally adjusted in the same way to assign calendar dates to the full year

7

166 data set.

167   Fig. 4 shows the environmental parameters used as forcing variables in the model. Daily temperature has been

168 measured at the water-sediment interface in the Roscanvel bank from 1998 until 2000. A linear regression between

169 registered temperature at Roscanvel and those from the SOMLIT probe in Sainte-Anne (data provided by "Service

170 d'Observation en Milieu Littoral, INSU-CNRS, Brest"), allowed the reconstruction of bottom temperature in Roscan-

171 vel between 2001 and 2003. Two food proxies have been monitored: the particulate organic matter (POM, in mg.l^{-1})

172 and the phytoplankton concentration (in cell.l^{-1}). These data come from an instrumented site which is monitored by

173 the REPHY network (PHYtoplankton and PHYcotoxins monitoring NEtwork, Ifremer). POM data in mg.l^{-1} were

174 transformed into a number of particles per liter by considering an average particle diameter of 30 μm (weight of

175 1.4 10^{-5}g for a density of 1) per POM particle. Environmental measurements were linearly interpolated to fit the time

176 step of the simulations.

177 *2.4. Model simulations*

178   Simulations were performed using GNU Octave software (Eaton et al., 2008). Initial state variables values are

179 obtained from observed measurements in the first sampling of the year (Table 2). A Eulerian integration method was

180 used to study the dynamics of each state variable in time. As the individuals are three-year-old and fully mature

181 (Antoine et al., 1979), the initial amount of maturity is taken to be equal to the maturity at puberty (supposed to be

182 maintained during the adult stage, Kooijman, 2010). Using the DEB model developed for *P. maximus* we simulated the

183 body dry weight, the shell height, the DSGR and the gonado-somatic index between 1998 and 2003. The evolution

184 of shell height over time has been simulated from the relationship: $V = (\delta_{\mathcal{M}} L_{Obs})^3$, where L_{Obs} is in cm. The

185 gonado-somatic index (GSI) was calculated as a ratio between the wet weight of reserves allocated to reproduction

186 (W_{E_R}) and the cubic shell length. Total body dry weight and GSI were calculated according to the formulas:

$$W \quad = V d_{Vd} + \left[(E + E_R) \frac{w_E}{\mu_E} \right] \tag{9}$$

$$GSI \quad = \frac{W_{E_R}}{Ls^3} 1000 \quad \text{with} \quad W_{E_R} = \frac{E_R \dfrac{w_E}{\mu_E}}{d_{Vd}} \tag{10}$$

187 where w_E is the molar weight of reserve (g.mol^{-1}), μ_E is the energy content of one gram of reserve (J.mol^{-1}) and

188 d_{Vd} is the wet weight to dry weight ratio.

189   In the DEB theory, strategies for handling the reproduction buffer and spawning are species-specific. In *P. maxi-*

190 *mus*, gamete releasing is asynchronous, partial and has been reported to be influenced by four parameters: temperature,

8

food density, a minimal GSI and photoperiod (Paulet et al., 1997; Saout et al., 1999; Barber and Blake, 2006). Sharp decreases observed in measured GSI can be correlated to spawning events. The model was then calibrated to fit GSI observations by taking into account the influence of these forcing variables. The first spawning event of the year in the Bay of Brest is usually synchronous with the first spring bloom (Paulet et al., 1997), thus a threshold in food density was set at $3 \ 10^5$ cells.L^{-1} (average value corresponding to a substantial resumption of primary production in spring) under which no spawning is possible. As for many bivalve species, temperature has a crucial influence on gametogenesis but also on the releasing of gametes. We decided to apply the day-degree concept as a trigger for spawning. Once the seawater has reached a threshold of 12 °C, daily cumulative degrees above this limit were counted and a value of 75 degree-days was found to be required to reach a condition ready for spawning. Then, a minimum GSI of 7 was put at the third trigger for spawning, accounting for a minimal advancement in gametogenesis. The reproduction buffer was then half emptied and the degree-days counter reseted. The last parameter, the photoperiod, is a key parameter that blocks the release of gamete so that after the fall equinox no spawning is ever possible (Devauchelle and Mingant, 1991; Duinker et al., 1999; Saout et al., 1999).

3. Results

3.1. DEB Parameters estimates

The DEB parameters estimated for *P. maximus* through the covariation method are presented in Table 3. The overall goodness of fit of model prediction to data on the great scallop's life history traits (Table 4) was evaluated at 8.72 over 10, with fit = 10 × (1 - mre). The only pattern not very well captured is the age at metamorphosis, known to be between 20 and 30 days and which is estimated in our model at about 10 days. An other evidence that there is a satisfactory correspondence between the simulations and the observations is to use a full life-cycle growth data set (Fig. 5), which shows the good prediction of the model. Primary DEB parameters for a given organism always correspond to those of an embryo and for the majority of species do not vary during life span. Nevertheless, some taxa, including *P. maximus*, experience a metabolic acceleration after metamorphosis causing a change in the value of some parameters. The maximum surface-specific assimilation rate $\{\dot{p}_{Am}\}$ and the energy conductance $\dot{v}$ would respectively increase to 282 J.d^{-1}.cm^{-2} and 0.063 cm.d^{-1} at this stage transition. As three-year-old individuals are modeled here, values after metamorphosis have been used for the following simulations.

3.2. Environmental forcing variables

Temperature monitored during a study period of six years follow a rather constant annual cycle (Fig. 4) with common winter values between 8 and 12 °C from December to February and from 15 to 19 °C during summer (July to

9

September). Noticeable peaks occurred in summer 2001 reaching a temperature of 19.7 °C as well as sharp drops until 8.4 °C during January 2003. POM concentration in the water column is very variable and no clear pattern is identified during the year. Still, tremendous peaks can be seen in May of the years 1998, 2001 and 2003 with values up to almost $8 \ 10^6$ particles per liter, contrasting with the range of variation observed during the rest of the year (between 1 and $3 \ 10^6$ particles per liter). The curve presented here is the result of the deduction of algal cell counting from the total POM measured by the SOMLIT station, thus strong decreases are also observable when phytoplankton blooms occur (e.g. in June, July and December 2000 or in August 2003). Finally, Fig. 4 shows a relatively high inter- and intra-annual variability in the counting of algal cells along the studied period. The lowest values are recorded in winter with values under 10^4 every year and the first bloom appears in a very irregular way. Indeed, in 1998, 2001 and 2002 the first phytoplanktonic bloom event occurred in late February-early March whereas in other years it is delayed and only occurs between mid-April and June (in 2000). An other interesting feature is the yearly average of phytoplankton cells concentration, allowing to distinguish highly productive years from unfruitful ones. It appears that 2002 would therefore have been the worst year with only 143,759 cells.L^{-1} followed by 1999 and 2003 with respectively 239,305 and 262,260 cells.L^{-1}. Then come the more productive years, 2001, 1998 with respectively 392,150 and 439,278 cells.L^{-1} and eventually, 2000, the most productive year in terms of phytoplankton cell concentration with about 504,592 cells.L^{-1}.

3.3. Feeding and food sources

Fig. 6 shows the functional responses f_X and f_Y, of the two food types respectively and the total f as the overall functional response of the scallop to the food supply. It pictures the alternation between the two food types available according to the period of the year. Phytoplanktonic concentration are very low until the end of winter and after mid fall (Fig. 4) whereas POM is present almost all the time. This results into a more elevated f_Y at the beginning and the end of the year which falls under 0.1 the rest of time, when phytoplankton cells are more present. The functional response to POM concentration never reaches levels above 0.5 and are mostly fluctuating between 0 and 0.4. In 1998, it was never over 0.2 and reached a maximum in October 2002. To the contrary, the f_X reaches high values almost all years during phytoplanktonic blooms, from 0.8 in June 2002 to May 0.99 in 2000 but is almost null in winter.

The two calibrated parameters in the simulations using the preference module were the maximum specific filtration rates F_{Xm} and F_{Ym}. They account for the amount of water cleared when food particles of each type are in the environment. F_{Xm} varied between 50 L.d^{-1}.cm^2, in 2001 and 100 L.d^{-1}.cm^2, in 2000 and F_{Ym} from 2 L.d^{-1}.cm^2, in 1998 to 4 L.d^{-1}.cm^2, in 1999. Most of the F_{Xm} were set around 50 L.d^{-1}.cm^2 and most of the F_{Ym} around 2 L.d^{-1}.cm^2. No clear relationship is found between values of F_{Xm} and F_{Ym} and the phytoplankton or POM concentration in the water. As for the value of X_K in the simulations using only phytoplankton, it ranged from 40,000 #.L^{-1}

in 2000 to 160,000 #.L^{-1} in 1998 and 2001.

3.4. Model simulation

Several physiological processes and life traits of three-year-old scallops were simulated using the DEB model from 1998 to 2003 in the Bay of Brest. Simulations of dry flesh weight are presented in Fig. 7. The model successfully captured the variations of dry weight along the seasons. Modeled weights using only one food proxy are less accurate than weight estimations resulting from the two-food-type assimilation module. The general pattern observed when the model is fed with one food source is an over-estimation in spring and autumn whereas at the end of the year, simulations often decrease too much compared to observations. Now concerning the simulations when both cell counting and POM are taken into account, a slight over-estimation in winter 1998 and 2000 is to be noticed, and a small under-estimation during winter 1999 too. The brutal weight losses that can be seen along the simulations account for spawning events which seem to have a rather low impact on the total body dry weight. Flesh growth is variable from one year to another but very similar between observed and simulated data: during year 2000, scallop dry weight increased of 4 g dry mass (5 g according to simulations) whereas in 2002 the gain in mass was only of 1.7 g dry weight (1.8 g according to simulations). The highest discrepancy between observed and simulated data is reached in 1998 as the model predicts a final dry weight 1.6 g heavier than the observations. That year, during the last months of growth, the observed weight loss (down to 8.5 g) was not reproduced as the model predicted a rather strong peak (11.2 g) in November. At the end of winter, scallops sometimes do not have enough energy in reserves and maintenance has to be paid from structural volume. The flesh dry weight can then loose few milligrams as it is observed between January and March 2001 and 2003 with a loss of 0.3 and 0.2 g dry weight respectively. The acceleration of growth rate from spring to mid-autumn is well reproduced every year, after which a decrease in the first months of winter is well simulated.

Shell growth was investigated in two complementary ways: (1) by examining the daily shell growth rate and (2) by looking at the cumulated growth in length. Fig. 8 shows the simulated DSGR for the six studied years. The observed data correspond to the cumulated average of DSGR measured on a sample of 10 individuals of the three-year age cohort of the studied year. The lowest measured DSGR was 20.3 μm.d^{-1} (in 2001) and the highest was 156.2 μm.d^{-1} (in 2003) whereas the simulated DSGR ranges from 1 to 91.7 μm.d^{-1}. Peaks of growth rate are hardly predicted but the simulated DSGR is still in the order of magnitude of the observations, except in 1998 and 2002 where a low growth is observed. Regarding the duration of the growing season, the simulations are in accordance with the observations. The resumption of shell growth is precisely captured by the model with an average time lag less than a week. An odd feature is observed during the first months of winter 1998, 1999, 2002 and 2003 where the model predicts a tiny growth in length (< 10 μm.d^{-1}) at a moment of dormancy for *P. maximus*.

11

The shell lengths presented in Fig. 9 correspond to the cumulated growth in length. Simulated growth can here be compared to the observations with an emphasis on the final size of the animal at the end of the growing season. Here again simulated shell length using phytoplankton only are less relevant than those using algae plus POM. Growth always seems to start earlier in simulated data than in observed ones, which relates to the precocious low DSGR observed previously at the beginning of the year (see Fig. 8) and not taken into account in the observed data. The total increase in shell length (the shell length produced during the year) is very well modeled, with a slightly longer distance in the predicted data (still less than 100 μm), ranging from 0.05 mm in 2003 to 1.5 mm in 1999 or 2001. Except for the year 2002, the slope of the predicted growth curve is extremely similar to the observed one.

The last biological trait studied is the gonado-somatic index (GSI), shown in Fig. 10. *P. maximus* from the Bay of Brest are known to spawn in a very variable way, regarding the intensity, the number and the timing of spawning events between individuals and years. Apart from a slight over-estimation at the end of years 1998 and 2001, the ratio of reproduction buffer over structure is rather well described by the model when the two food descriptors are taken into account. If only phytoplankton is considered, more decreasing periods are observed like in spring 1999, 2001 or autumn 2002, which does not match the observed data at these moments. The timing of the first spawning event is accurately reproduced in the simulation (a little less when using only one food proxy). The spawning efficiency parameter set at 0.5, meaning that the gonad is half-flushed during spawning, seems to be a relevant value since the simulated GSI do not fall below the lower bound observed.

The model response was also tested by the simulation of an average individual from its birth until several years of growth along the study period. Fig. 11 presents the growth curve of a great scallop born in June 1998 that lived five years in the Bay of Brest (environmental variables were the same as those used in previous simulations). Predictions made by the model are very realistic, producing a five-year-old scallop of 11 cm with a very low growth rate at this age, which closely matches observations. Finally, a last property of the model was highlighted by plotting DSGR data both observed and simulated against environmental variables to look at the effects of forcing parameters on growth. Fig. 12 shows for years 1999 and 2001 that simulated DSGR is strongly forced by bottom temperature. Functional response and thus food availability have minor effect on the modeled growth while it appears to be more determining when looking at the measured DSGR. This particularly holds true when the feeding response shows sharp decreases like in June 1999 or late August 2001.

12

4. Discussion

4.1. Modeling the life-cycle of P. maximus

In this study, we used DEB theory to build a mechanistic bioenergetic model for *P. maximus* in the Bay of Brest, including a detailed formulation of the ingestion and food handling processes through the SU concept. The set of estimated parameters allowed us to reproduce the growth of an average great scallop individual during its entire life-cycle with a satisfying accuracy (Fig. 5). The age at metamorphosis was the only life trait that did not fit very well (Table 4), despite the addition of the acceleration module (Kooijman et al., 2011) to the standard DEB model. It may be linked to the low accuracy of the determination of age, size and weight at sexual maturity. This maturity level is reported through the literature to be reached during the second year of life (Mason, 1957; Pazos et al., 1997; Chauvaud et al., 1998). A more precise knowledge of the timing of this critical life trait would certainly allow to capture more efficiently the characteristics of other development stages.

The model was tested in the well studied environment of the Bay of Brest during six years of environmental monitoring and scallop sampling. Model predictions sometimes showed less good correspondence with measured data, like in 2002 when DSGR was hardly simulated, or at the end of the year 1998 when an over-estimation of dry weight is detected. It has to be noted that daily increments under 50 μm are very difficult to measure under binocular magnifier which tend to reduce the observed number of truly formed increments and the minimal size of striae observed. The model sometimes predicted slightly longer shell height which can easily be explain by the fact that archived shells have been manipulated many times causing damages to the ventral margin of the shell, i.e. the latest increments formed, which can have been abraded. But in a general way, the various physiological traits simulated in three-year-old individuals in the Bay of Brest were very similar to the observations made on wild population during this period.

All simulations presented here were made over one year and for individuals that belong to three-year age cohort, which correspond to an age between 2.5 and 3.5 years old. An interesting question is how the model behave in the long term, when scallops are grown from the egg to an advanced age. Fig. 11 shows that when the simulated animal reaches three years old in 2001 it can be compared to observations made this year on scallops of the same year-class (Fig. 8 and 9). Here again we see that this long term simulation is in accordance with observations.

4.2. Growth and feeding

An interesting pattern is that simulated DSGR is strongly impacted by bottom temperature, as shown in Fig. 12. This is in accordance with works of Chauvaud et al. (1998) who highlighted the major role of thermal conditions in normal growth variations (95 % of the variability explained by this factor). It is also in accordance with the DEB theory

13

and more generally with the Arrhenius relationship. This law states that all physiological rates, including the energy flux allocation from reserve to shell production (i.e. structure), are impacted by temperature. Concerning growth anomalies and short term variations in shell growth, it has been established that food was one the most triggering factor (Chauvaud et al., 1998; Lorrain et al., 2000). This pattern was not very well captured by the model compared to measured DSGR (Fig. 12). In 1999, scallops shown a daily growth divided in three periods: (1) a low start around 50 μm per day during few weeks, (2) then a sharp increase to more elevated values close to 90 μm per day with two peaks reaching 140 μm per day and (3) a progressive decrease punctuated with small and short peaks until a definitive stop in early October. The same profile was observed on one-year-old scallops by Lorrain et al. (2000) for the same year. To the contrary, the model predicts a rather smoother growth along the growing period (which has still the same duration and timing), with a DSGR rapidly reaching a plateau around 70 μm and starting to decrease two months later than the observations but at a faster rhythm.

One objective of this work was to test the hypothesis of a selective ingestion of *P. maximus* between two substrates. When looking at the functional responses of the modeled individuals (Fig. 6), we see that f_X reaches high values almost all years during phytoplanktonic blooms. To the contrary, f_Y is rather low all along the year, which tends to confirm our guess. The maximum specific filtration rate for phytoplankton cells (F_{Xm}), which was calibrated to fit the observed data, varied between 25 and 100 l.d^{-1}.cm^2 respectively. This corresponds to values of 11 l.h^{-1} and 44 l.h^{-1} per individual, which is in accordance with literature values (Shumway and Parsons, 2006; Strohmeier et al., 2009; Cranford et al., 2011). On the other hand, F_{Ym} varies at a far more lower level, between 2 and 4 l.d^{-1}.cm^2. This clearly indicates that substrate X (phytoplankton cells) is positively selected compared to substrate Y (rest of POM), which confirms our hypothesis. It is relatively easy to understand this when considering the high energetic quality of fresh phytoplankton cells compared to suspended matter, which includes organic debris (Alber and Valiela, 1996). The use of the POM proxy as a second food source, yet under-selected, shown its benefits compared to simple diet simulations. POM seems to be an additional food source allowing scallops to compensate phytoplankton limitation between algae blooms. Indeed some studies already shown evidences of organic aggregates and flocs assimilation in scallops, although less efficiently than phytoplankton (Alber and Valiela, 1996; MacDonald et al., 2006).

Even if the maximum specific filtration rate is in compliance with already reported data, one can see that its variation range is rather large. Although the model is entirely deterministic, we still face the fact that the filtration rate is obtained by calibration, as it used to be the case with the half-saturation constant in previous DEB models. Possible reasons for such differences among years might rely on the inter-individual variability. Indeed, animals collected at the very same moment and selected in the same year class shown considerable heterogeneity in biometric measurements (see the confidence intervals of observed data on Fig. 7 and 10). Moreover, consequent amounts of inorganic particles

14

from riverine inputs are discharged in the Bay of Brest and could also cause annual variations in the mean filtration rate. Indeed, filtration rates of filter feeding bivalves are negatively impacted by these non-edible particles inputs, which compete with food particles (Kooijman, 2006; Saraiva et al., 2011b). To improve the determinism in the maximum specific filtration rate estimation and avoid calibration steps two conditions are required: 1) integrate the effect of non-edible particles via a third substrate for SUs as done by Saraiva et al. (2011b), 2) include feeding experiment data into the parameter estimation procedure to better determine filtration and ingestion rates parameters.

A recurrent issue in individual bioenergetic modeling is the choice of a good food proxy. Some studies using DEB theory to model bivalve bioenergetics have already raised this problem (Pouvreau et al., 2006; Bourlès et al., 2009; Rosland et al., 2009). Bourlès et al. (2009) tested different types of trophic markers like particulate organic matter, particulate organic carbon, chlorophyll a concentration and phytoplankton enumeration. It came out that chl-a concentration, albeit being easily monitored, was not sufficient to capture all the variations observed in the physiological processes studied. On the other hand, they showed that microalgae expressed in cell number per liter should be considered as a better food marker. This approach worked efficiently for *C. gigas* and also seems to be relevant for *P. maximus*. Fig. 12 also shows that the simulated ingestion represented by the functional response is in accordance with the observed DSGR, except in early August 2001 when no growth increase is observed whereas the model shows a rather high ingestion.

Deviations between the model and data that might be addressed by a better descriptor of the trophic source that would integrate food quality. Indeed, Lorrain et al. (2000) have shown that the DSGR of one-year-old scallops in the Bay of Brest could be negatively impacted by the presence of some phytoplanktonic species such as diatoms *Ceratolina pelagica* or *Rhizosolenia delicatula*, responsible of short drops in the daily growth of these animals in early May 1998 and 1999. However, since we used individuals from the three-year age cohort who started their shell growth later in the year due to their age (late May and June respectively), we did not observed such effects. Moreover, DSGR of three-year-old scallops is two times lower than in younger individuals. It is thus difficult to see the variation of ingestion according to food biomass from the DSGR profiles in our study. A perspective to the present study could consist in testing differential ingestion rates for *P. maximus* when the phytoplanktonic biomass is dominated by some algae species during crucial period of the growing season (e.g. when the great scallop is also about to start to reproduce and complete its gamete maturation).

4.3. Reproduction

Modelling reproductive activity is not a simple task, especially for *P. maximus*, an asynchronous spawner that only flush partially its gonad during highly variable spawning events. DEB theory do not specify how to handle reproductive effort in a general way, each species needs a specific implementation. In our model, spawning triggering

15

requires data that are already necessary to run a DEB model (temperature and food) plus a photoperiod sinusoid. It is well known that parameters potentially bringing about gamete release in scallops are numerous, including temperature, food availability, photoperiod but also lunar phase, salinity, dissolved oxygen, pH, mechanical shocks and ectocrines (Barber and Blake, 2006). Therefore, we were motivated to take into account the most recognized factors. The resulted simulated GSI is acceptable as it reproduces the general pattern of gonad dynamics (Fig. 10). The predicted start of gametogenesis in winter matches the observed data, except in 1998 and 2001, where the increase of the simulated index is not as sharp as in the observations. During winter, energy stored in the reproduction buffer E_R is not only used to produce gametes but also to meet maintenance requirements if reserves are not sufficient to do so under seasonal starvation. The fact that this energy would be used for two different processes during the same period (Mason, 1957; Lorrain et al., 2002) might explain the general under-estimation observed at the beginning of the winter. A study of the biological cycles of *P. maximus* realized by Paulet et al. (1997) brings another look on the mechanisms involved in the compartment dynamics. Paulet and co-workers described the complex evolution of the gonad in relation to somatic tissues along the year. They showed that gametogenesis presented a stop in October and November, another one at the end of the winter and a maximum gametic production period in April and May. This is consistent with our results except for the late autumn stop. As non-emitted gametes during spawning events are resorbed and eliminated during fall, they provide energy to other tissues thanks to atresia (Le Pennec et al., 1991). Exploring this phenomenon in more details could improve the simulation of reproductive effort of *P. maximus* at the end and the beginning of the year (but at the expense of the model simplicity). Eventually, the mismatch between simulated and observed data in early 1998 and 2001 might also suffer from a rather elevated value of κ (0.86) compared to other bivalve species such as the Pacific oyster (0.45 in van der Veer et al., 2006) or the blue mussel (0.67 in Saraiva et al., 2011a; 0.45 in Rosland et al., 2009).

Bernard et al. (2011) tried to improve the implementation of the reproductive effort in the DEB model of *C. gigas* in relation to environmental conditions. They adopted an approach involving the creation of a new state variable (the gonad structure) plus three additional parameters, while using derivatives of temperature as signals to begin and end the gametogenesis. However, those manipulations did not significantly addressed the bad fit of simulated gamete releases compared to observed data. Moreover they reported only one spawning event for *C. gigas* whereas several ones are clearly identified in *P. maximus* biological cycle, which may reduce the difficulty to accurately simulate it. One of their conclusion was to put more emphasis on the intake of energy rather than on the reproductive activity. But finally, when looking at these two studies, one focusing on the reproductive effort modelling and ours on the feeding modelling, results are sensitively the same.

To finish, one step not yet reached by this model is the simulation of the number of gametes emitted. In the current

16

state, our model considers that the flux of reserve $\dot{p}_R$ is used either for maturation (when in the juvenile stage) or to fuel the reproduction buffer (after reaching the adult stage) from which gamete production is realized. Modeled reserves in the reproduction buffer are not necessarily used immediately for gamete production. This has a repercussion in the simulation of this index, which can show a too great increase at the end of the year (especially in 1998 and 2001) compared to the field data. This could be explained by two means. First, it is possible that a very late spawning event occurred, outside the generally expected period in this location (from May to July, Paulet et al., 1997). Incidentally, this late spawning would probably not be significant for the population growth, since larvae hatching at this period of the year would hardly survive to bad food condition of autumn. The second possible cause relies on the already invoked atresia hypothesis. This phenomenon is not integrated into the model and would require additional parameters. In order to keep a relatively low complexity level of the model and because this physiological process was already rather well simulated (our estimations are still in the confidence range of the data variability) we did not implemented this pattern into the model.

4.4. Conclusions and perspectives

In this study we implemented a DEB model for the great scallop, *P. maximus*, in the Bay of Brest using the Synthesizing units concept to model energy acquisition. Primary parameters were obtained by the covariation method for parameters estimation, producing estimates able to reproduce life-cycle history traits with still a slight underestimation of the age at metamorphosis. Various physiological processes such as growth in weight, shell growth or reproductive activity were accurately modeled and successfully matched observation data over a six-years study. To complete the validation of this model we need to test the set of parameters on an other population living in a relatively different environment such as the cold and eutrophic fjords of Norway for instance.

Results of this work showed that assimilation even if well implemented in the model still requires some improvement and a deeper reflection, especially concerning the trophic input. We did not addressed the issue of the determinism of energy input as the maximum filtration rate still requires a calibration. However we brought tools to develop and improve the way feeding of filter feeders is formalized within DEB theory. Saraiva et al. (2011b) went further deep into the description of filtration, ingestion and assimilation processes in mussels *M. edulis*. By taking into account silts as an other potential substrate for SU, they were able to describe these processes through a DEB model, considering the effect of non-edible particles on energy allocation. As the Bay of Brest receives high riverine inputs from two rivers and underwent a recent invasion by the slipper limpet *Crepidula fornicata* causing a significant silting up of the bay's sea-floor (Thouzeau et al., 2002), it would be interesting to look at the response of the model when fueled by both organic and inorganic matter.

17

It has long been suspected that filter feeders and especially *P. maximus* could be able to select algae cell types according to their chemotactile attractiveness, size or shape (Raby et al., 1997; Ward and Shumway, 2004). The state of freshness of phytoplankton cells might also be critical so efforts should be deployed to find food markers able to describe the quality of the trophic resource. Moreover, recent works have reaffirmed through isotopic analysis the presence in *P. maximus*'s diet of bacteria (Nerot et al., 2012). It must also be interesting to look at this feature but certainly much more difficult to assess the bacterial biomass in the environment.

Acknowledgements

References

Alber, M., Valiela, I., 1996. Utilization of microbial organic aggregates by bay scallops, *Argopecten irradians* (Lamarck). Journal of experimental marine biology and ecology 195 (1), 71–89.

Alunno-Bruscia, M., Bourlès, Y., Maurer, D., Robert, S., Mazurié, J., Gangnery, A., Goulletquer, P., Pouvreau, S., 2011. A single bio-energetics growth and reproduction model for the oyster *Crassostrea gigas* in six Atlantic ecosystems. Journal of Sea Research 66 (4), 340–348.

Antoine, L., Garen, P., Lubet, P., 1979. Conséquences sur la maturation et la croissance d'une transplantation de naissain de *Pecten maximus* (L.). Cahiers de Biologie Marine (Station Biologique de Roscoff) 20 (2), 139–150.

Bachok, Z., Meziane, T., Mfilinge, P. L., Tsuchiya, M., 2009. Fatty acid markers as an indicator for temporal changes in food sources of the bivalve *Quidnipagus palatum*. Aquatic Ecosystem Health & Management 12 (4), 390–400.

Barber, B. J., Blake, N. J., 2006. Reproductive physiology. In Scallops: Biology, Ecology and Aquaculture. Vol. 35. Elsevier, Developments in aquaculture and fisheries science, Ch. 8, pp. 357–416.

Bayne, B. L., Hawkins, A. J. S., Navarro, E., 1987. Feeding and digestion by the mussel *Mytilus edulis* L. (Bivalvia: Mollusca) in mixtures of silt and algal cells at low concentrations. Journal of Experimental Marine Biology and Ecology 111 (1), 1–22.

Bernard, I., de Kermoysan, G., Pouvreau, S., 2011. Effect of phytoplankton and temperature on the reproduction of the Pacific oyster *Crassostrea gigas*: Investigation through DEB theory. Journal of Sea Research 66 (4), 349–360.

Bourlès, Y., Alunno-Bruscia, M., Pouvreau, S., Tollu, G., Leguay, D., Arnaud, C., Goulletquer, P., Kooijman, S. A. L. M., 2009. Modelling growth and reproduction of the Pacific oyster *Crassostrea gigas*: Advances in the oyster-DEB model through application to a coastal pond. Journal of Sea Research 62 (2–3), 62–71.

Buestel, D., Cochard, J.-C., Dao, J.-C., Gérard, A., 1982. Production artificielle de naissain de coquilles Saint-Jacques *Pecten maximus* (L.). Premiers résultats en rade de Brest. Vie Marine - Annales de la Fondation océanographique Ricard 4, 24–28.

Cardoso, J. F. M. F., Witte, J. I. J., van der Veer, H. W., 2006. Intra- and interspecies comparison of energy flow in bivalve species in Dutch coastal waters by means of the Dynamic Energy Budget (DEB) theory. Journal of Sea Research 56 (2), 182–197.

Chauvaud, L., Donval, A., Thouzeau, G., Paulet, Y.-M., Nézan, E., 2001. Variations in food intake of *Pecten maximus* (L.) from the Bay of Brest (France): Influence of environmental factors and phytoplankton species composition. Comptes Rendus de l'Académie des Sciences - Series III - Sciences de la Vie 324 (8), 743–755.

Chauvaud, L., Patry, Y., Jolivet, A., Cam, E., Le Goff, C., Strand, Ø., Charrier, G., Thébault, J., Lazure, P., Gotthard, K., Clavier, J., 2012. Variation in size and growth of the great scallop *Pecten maximus* along a latitudinal gradient. PLoS ONE 7 (5), e37717.

Chauvaud, L., Thouzeau, G., Paulet, Y.-M., 1998. Effects of environmental factors on the daily growth rate of *Pecten maximus* juveniles in the Bay of Brest (France). Journal of Experimental Marine Biology and Ecology 227 (1), 83–111.

Comely, C. A., 1974. Seasonal variations in the flesh weights and biochemical content of the scallop *Pecten maximus* (L.) in the Clyde Sea area. Journal du Conseil 35 (3), 281–295.

Cranford, P. J., Ward, J. E., Shumway, S. E., 2011. Bivalve filter feeding: variability and limits of the aquaculture biofilter. In Shellfish aquaculture and the environment. Wiley-Blackwell, Hoboken, NJ, pp. 81–124.

Devauchelle, N., Mingant, C., 1991. Review of the reproductive physiology of the scallop, *Pecten maximus*, applicable to intensive aquaculture. Aquatic Living Resources 4 (1), 11.

Duinker, A., Saout, C., Paulet, Y.-M., 1999. Effect of photoperiod on conditioning of the great scallop. Aquaculture International 7 (6), 449–457.

Eaton, J. W., Bateman, D., Hauberg, S., 2008. GNU Octave Manual Version 3. Network Theory Limited.

Flye-Sainte-Marie, J., Jean, F., Paillard, C., Ford, S. E., Powell, E., Hofmann, E., Klinck, J., 2007. Ecophysiological dynamic model of individual growth of *Ruditapes philippinarum*. Aquaculture 266 (1–4), 130–143.

Freitas, V., Cardoso, J. F. M. F., Santos, S., Campos, J., Drent, J., Saraiva, S., Witte, J. I. J., Kooijman, S. A. L. M., van der Veer, H. W., 2009. Reconstruction of food conditions for northeast atlantic bivalve species based on dynamic energy budgets. Journal of Sea Research 62 (2–3), 75–82.

Gruffydd, L. D., Beaumont, A. R., 1972. A method for rearing *Pecten maximus* larvae in the laboratory. Marine Biology 15 (4), 350–355.

Heral, M., 1989. Traditional oyster culture in France. In: Barnabe Aquaculture. Ellis Horwood, pp. 342–387.

Kamermans, P., 1994. Similarity in food source and timing of feeding in deposit- and suspension-feeding bivalves. Mar. Ecol. Prog. Ser 104, 63–75.

Kooijman, S. A. L. M., 1998. The Synthesizing Unit as model for the stoichiometric fusion and branching of metabolic fluxes. Biophysical Chemistry 7 (1–2), 179–188.

Kooijman, S. A. L. M., 2006. Pseudo-faeces production in bivalves. Journal of Sea Research 56 (2), 103–106.

Kooijman, S. A. L. M., 2010. Dynamic Energy Budget theory for metabolic organization, cambridge, uk: cambridge Edition. University Press.

Kooijman, S. A. L. M., 2013. The evolution of metabolic acceleration in animals.

Kooijman, S. A. L. M., Pecquerie, L., Augustine, S., Jusup, M., 2011. Scenarios for acceleration in fish development and the role of metamorphosis. Journal of Sea Research 66 (4), 419–423.

Laing, I., 2000. Effect of temperature and ration on growth and condition of king scallop *Pecten maximus* spat. Aquaculture 183 (3–4), 325–334.

Laing, I., 2002. Effect of salinity on growth and survival of king scallop spat *Pecten maximus*. Aquaculture 205 (1–2), 171–181.

Laing, I., 2004. Filtration of king scallops *Pecten maximus*. Aquaculture 240 (1–4), 369–384.

Langdon, C. J., Newell, R. I. E., 1990. Utilization of detritus and bacteria as food sources by two bivalve suspension-feeders, the oyster *Crassostrea virginica* and the mussel *Geukensia demissa*. Mar. Ecol. Prog. Ser 58, 299–310.

Le Pennec, M., Beninger, P. G., Dorange, G., Paulet, Y.-M., 1991. Trophic sources and pathways to the developing gametes of *Pecten maximus* (Bivalvia: Pectinidae). Journal of the Marine Biological Association of the United Kingdom 71, 451–463.

Le Pennec, M., Paugam, A., Le Pennec, G., 2003. The pelagic life of the pectinid *Pecten maximus* - a review. ICES Journal of Marine Science: Journal du Conseil 60 (2), 211–233.

534   Lika, K., Kearney, M. R., Freitas, V., van der Veer, H. W., van der Meer, J., Wijsman, J. W. M., Pecquerie, L., , Kooijman, S. A. L. M., 2011. The

535   "covariation method" for estimating the parameters of the standard Dynamic Energy Budget model I: Philosophy and approach. Journal of Sea

536   Research 66 (4), 270–277.

537   Lorrain, A., Paulet, Y.-M., Chauvaud, L., Savoye, N., Donval, A., Saout, C., 2002. Differential delta13C and delta15N signatures among scallop

538   tissues: implications for ecology and physiology. Journal of Experimental Marine Biology and Ecology 275 (1), 47–61.

539   Lorrain, A., Paulet, Y.-M., Chauvaud, L., Savoye, N., Nézan, E., Guérin, L., 2000. Growth anomalies in *Pecten maximus* from coastal waters (Bay

540   of Brest, France): relationship with diatom blooms. Journal of the Marine Biological Association of the UK 80 (04), 667–673.

541   MacDonald, B. A., Bricelj, M. V., Shumway, S. E., 2006. Physiology: Energy acquisition and utilisation. In Scallops: Biology, Ecology and

542   Aquaculture. Vol. 35. Elsevier, Developments in Aquaculture and Fisheries Science, Ch. 7, pp. 417–492.

543   Marín Leal, J. C., Dubois, S., Orvain, F., Galois, R., Blin, J.-L., Ropert, M., Bataillé, M.-P., Ourry, A., Lefebvre, S., 2008. Stable isotopes (delta13C,

544   delta15N) and modelling as tools to estimate the trophic ecology of cultivated oysters in two contrasting environments. Marine Biology 153 (4),

545   673–688.

546   Mason, J., 1957. The age and growth of the scallop, *Pecten maximus* (L.), in Manx waters. Journal of the Marine Biological Association of the

547   United Kingdom 36 (03), 473–492.

548   Nerot, C., Lorrain, A., Grall, J., Gillikin, D. P., Munaron, J.-M., Le Bris, H., Paulet, Y.-M., 2012. Stable isotope variations in benthic filter feeders

549   across a large depth gradient on the continental shelf. Estuarine, Coastal and Shelf Science 96, 228–235.

550   Paulet, Y.-M., Bekhadra, F., Devauchelle, N., Donval, A., Dorange, G., 1997. Seasonal cycles, reproduction and oocyte quality in *Pecten maximus*

551   from the Bay of Brest. Annales de l'Institut océanographique 73 (1), 101–112.

552   Paulet, Y.-M., Fifas, S., 1989. Etude de la fécondité potentielle de la coquille Saint-Jacques *Pecten maximus*, en baie de Saint-Brieuc. Haliotis 19,

553   275–285.

554   Pazos, A. J., Román, G., Acosta, C. P., Abad, M., Sánchez, J. L., 1997. Seasonal changes in condition and biochemical composition of the scallop

555   *Pecten maximus* (L.) from suspended culture in the Ria de Arousa (Galicia, N.W. Spain) in relation to environmental conditions. Journal of

556   Experimental Marine Biology and Ecology 211 (2), 169–193.

557   Pouvreau, S., Bourlès, Y., Lefebvre, S., Gangnery, A., Alunno-Bruscia, M., 2006. Application of a dynamic energy budget model to the Pacific

558   oyster, *Crassostrea gigas*, reared under various environmental conditions. Journal of Sea Research 56 (2), 156–167.

559   Raby, D., Mingelbier, M., Dodson, J. J., Klein, B., Lagadeuc, Y., Legendre, L., 1997. Food-particle size and selection by bivalve larvae in a

560   temperate embayment. Marine Biology 127, 665–672.

561   Ren, J. S., Ross, A. H., 2005. Environmental influence on mussel growth: A dynamic energy budget model and its application to the greenshell

562   mussel *Perna canaliculus*. Ecological Modelling 189 (3–4), 347–362.

563   Robert, R., Moal, J., Campillo, M.-J., Daniel, J.-Y., 1994. The food value of starch rich flagellates for *Pecten maximus* (L.) larvae. Preliminary

564   results. Haliotis 23, 169–710.

565   Rosland, R., Strand, Ø., Alunno-Bruscia, M., Bacher, C., Strohmeier, T., 2009. Applying Dynamic Energy Budget (DEB) theory to simulate growth

566   and bio-energetics of blue mussels under low seston conditions. Journal of Sea Research 62 (2–3), 49–61.

567   Rossi, F., Herman, P. M. J., Middelburg, J. J., 2004. Interspecific and intraspecific variation of delta13C and delta15N in deposit- and suspension-

568   feeding bivalves (*Macoma balthica* and *Cerastoderma edule*): Evidence of ontogenetic changes in feeding mode of *Macoma balthica*. Limno-

569   logy and Oceanography 49 (2), 408–414.

570   Samain, J. F., Cochard, J. C., Chevolot, L., Daniel, J. Y., Jeanthon, C., Le Coz, J. R., Marty, Y., Moal, J., Prieur, D., Salaun, M., 1986. Effect of sea

571   water quality on larval growth of *Pecten maximus* in a hatchery: preliminary results. Haliotis 16, 363–381.

572   Saout, C., Quéré, C., Donval, A., Paulet, Y.-M., Samain, J.-F., 1999. An experimental study of the combined effects of temperature and photoperiod

on reproductive physiology of *Pecten maximus* from the Bay of Brest (France). Aquaculture 172 (3–4), 301–314.

Saraiva, S., van der Meer, J., Kooijman, S. A. L. M., Sousa, T., 2011a. DEB parameters estimation for *Mytilus edulis*. Journal of Sea Research 66 (4), 289–296.

Saraiva, S., van der Meer, J., Kooijman, S. A. L. M., Sousa, T., 2011b. Modelling feeding processes in bivalves: A mechanistic approach. Ecological Modelling 222 (3), 514–523.

Shumway, S. E., Parsons, G. J., 2006. Scallops: Biology, Ecology and Aquaculture, Sandra E. Shumway and G. Jay Parsons Edition. Developments in Aquaculture and Fisheries Science, volume 35.

Strohmeier, T., Strand, Ø., Cranford, P., 2009. Clearance rates of the great scallop *Pecten maximus* and blue mussel *Mytilus edulis* at low natural seston concentrations. Marine Biology 156 (9), 1781–1795.

Thomas, Y., Mazurié, J., Alunno-Bruscia, M., Bacher, C., Bouget, J.-F., Gohin, F., Pouvreau, S., Struski, C., 2011. Modelling spatio-temporal variability of *Mytilus edulis* (L.) growth by forcing a dynamic energy budget model with satellite-derived environmental data. Journal of Sea Research 66 (4), 308–317.

Thouzeau, G., Chauvaud, L., Clavier, J., Donval, A., Guerin, L., Jean, F., Le Hir, M., Lorrain, A., Marc, R., Paulet, Y.-M., Raffin, C., Richard, J., Richard, M., 2002. La crépidule : identifier les mécanismes de sa prolifération et caractériser ses effets sur le milieu pour envisager sa gestion (Chantier : Rade de Brest). Tech. rep.

Troost, T. A., Wijsman, J. W. M., Saraiva, S., Freitas, V., 2010. Modelling shellfish growth with dynamic energy budget models: an application for cockles and mussels in the Oosterschelde (Southwest Netherlands). Philosophical Transactions of the Royal Society B: Biological Sciences 365 (1557), 3567–3577.

van der Veer, H. W., Cardoso, J. F. M. F., van der Meer, J., 2006. The estimation of DEB parameters for various Northeast Atlantic bivalve species. Journal of Sea Research 56 (2), 107–124.

Ward, J. E., Shumway, S. E., 2004. Separating the grain from the chaff: particle selection in suspension- and deposit-feeding bivalves. Journal of Experimental Marine Biology and Ecology 300 (1–2), 83–130.

Wijsman, J. W. M., Smaal, A. C., 2013. Growth of cockles (*Cerastoderma edule*) in the Oosterschelde described by a Dynamic Energy Budget model. Journal of Sea Research 66, 372–380.

Yokoyama, H., Sakami, T., Ishihi, Y., 2009. Food sources of benthic animals on intertidal and subtidal bottoms in inner Ariake Sound, southern Japan, determined by stable isotopes. Estuarine, Coastal and Shelf Science 82 (2), 243–253.

Tables

TABLE 1: Equations for the calculations of the variables of the *P. maximus* energy budget model

Name of the variable	Symbol	Unit	Equation
Reserve density	$[E]$	J.cm^{-3}	$= \dfrac{E}{V}$
Assimilation rate	$\dot{p}_A$	J.d^{-1}	$= \dot{J}_{EA}\,\mu_E\,V^{2/3}$
Mobilization rate	$\dot{p}_C$	J.d^{-1}	$= \dfrac{[E]}{[E_G] + \kappa[E]}\left(\dfrac{E_G\,\dot{v}}{V^{1/3}} + [\dot{p}_M]\right)$
Somatic maintenance	$\dot{p}_M$	J.d^{-1}	$= [\dot{p}_M]\,V$
Maturity maintenance coefficient	$\dot{p}_J$	J.d^{-1}	$= E_H\,k_J$
Structural growth	$\dot{p}_G$	J.d^{-1}	$= max(0, \kappa\,\dot{p}_C - \dot{p}_M)$
Allocation to reproduction buffer	$\dot{p}_R$	J.d^{-1}	$= max(0, (1-\kappa)\,\dot{p}_C - \dot{p}_J)$
Shrink to pay somatic maintenance	$\dot{p}_{S1}$	J.d^{-1}	$= max(0, \dot{p}_M - \kappa\,\dot{p}_C)$
Shrink to pay maturity maintenance	$\dot{p}_{S2}$	J.d^{-1}	$= max(0, \dot{p}_J - (1-\kappa)\,\dot{p}_C)$
Resorption of gonad	$\dot{p}_{RS}$	J.d^{-1}	$= \dfrac{\dot{p}_R\,\kappa_R + E_R\,\dfrac{1}{dt}}{\kappa_R}$
Lysis of structure	$\dot{p}_{VS}$	J.d^{-1}	$= \dfrac{(\dot{p}_{S1} + \dot{p}_{S2}) - \dot{p}_{RS}\,\kappa_R)\,d_{Vd}}{\kappa_R\,\mu_E)}$

TABLE 2: Initial value calculation of state variables in the DEB model of *P. maximus*.

$$\begin{aligned}
&\left.\begin{array}{l} L_i \\ W_i \end{array}\right\} \quad \text{Observed measurements in the first sampling of the year} \\[4pt]
&V_i = (L_i\,\delta_{\mathcal{M}})^3 \\[4pt]
&E_i = \frac{\{\dot{p}_{Am}\}}{\dot{v}}\,V_i \\[4pt]
&E_{Ri} = \left(W_i - V_i\,k_w - \left\{E_i\,\frac{w_E}{\mu_E}\right\}\right)\left(\frac{\mu_E}{w_E}\right) \\[4pt]
&E_{Hi} = E_H^p
\end{aligned}$$

TABLE 3: List of the parameters implemented in the DEB model of *P. maximus*. *Denotes estimated parameters using the coveriation method (Lika et al., 2011), other parameters have been calculated or fixed.

Description	Symbol	Value	Unit
Feeding process			
Number of moles per one X-type food particle	M_X	$1.05\ 10^{-10}$	mol
Number of moles per one Y-type food particle	M_Y	$2.49\ 10^{-9}$	mol
Maximum specific filtration rate of X-type particle	$F_X m$	$25 - 100$	l.d^{-1}.cm^2
Maximum specific filtration rate of Y-type particle	$F_Y m$	$2 - 4$	l.d^{-1}.cm^2
Binding rate of X-type particle	$\dot{b}_{XY}$	$= F_X m$	l.d^{-1}.cm^2
Binding rate of Y-type particle	$\dot{b}_{YX}$	0	l.d^{-1}.cm^2
Yield of reserve on X-type particle	y_{EX}	0.7	mol/mol
Yield of reserve on Y-type particle	y_{EY}	0.4	mol/mol
Primary parameters			
Shape coefficient*	$\delta_{\mathcal{M}}$	0.36	–
Fraction of mobilised reserve allocated to soma*	κ	0.86	–
Fraction of reproduction energy fixed in eggs*	κ_R	0.95	–
Energy conductance*	$\dot{v}$	0.021	cm.d^{-1}
Volume–specific maintenance costs*	$[\dot{p}_M]$	33.52	J.cm^{-3}
Volume–specific costs for structure*	$[E_G]$	2959	J.cm^{-3}
Maximum surface–specific assimilation rate*	$\{\dot{p}_{Am}\}$	94	J.d^{-1}.cm^{-2}
Maturity maintenance coefficient	k_J	0.002	1.d^{-1}
Maturity at birth*	$E_H{}^b$	0.00028	J
Maturity at metamorphosis*	$E_H{}^m$	0.0078	J
Maturity at puberty*	$E_H{}^p$	3000	J
Compound parameters			
Maximum reserve density	$[E_m]$	4483	J.cm^{-3}
Chemical potential of reserve	μ_E	474400	J.mol^{-1}
Molecular weight of reserve	w_E	23.9	g.mol^{-1}
Wet weight to dry weight ratio	d_{Vd}	0.12	–
Arrhenius temperature			
Reference temperature (arbitrary)	T_1	293	K
Arrhenius temperature	T_A	8990	K
Lower boundary of tolerance range	T_L	273	K
Rate of decrease at lower boundary	T_{AL}	50000	K

Data	Literature value	Predicted value	Reference
age at birth	2 d	1.795 d	[1]
age at metamorphosis	25 d	9.563 d	[1], [2]
age at puberty	during the second year	464.3 d	[1], [3], [4], [5]
physical length at birth	0.008 cm	0.007313 cm	[1], [2]
physical length at metamorphosis	0.024 cm	0.02867 cm	[1], [2], [5]
physical length at puberty	4 cm	4.426 cm	[1], [5]
ultimate physical length	12 cm	11.9 cm	[6]
dry weight at birth	$1 \, 10^{-7}$ g	$1.452 \, 10^{-7}$ g	[7]
dry weight at metamorphosis	$3 \, 10^{-6}$ g	$4.030 \, 10^{-6}$ g	[8]
dry weight at puberty	1 g	1.022 g	Chauvaud, pers. com.
ultimate dry weight	20 g	19.85 g	[9]
maximum reprod rate	$5.753 \, 10^4$ eggs per spawning	$4.227 \, 10^4$	[10]

Figure Captions

FIGURE 1. Conceptual scheme of the DEB model applied to the scallop *P. maximus*. Forcing variables (food and temperature) are in gray ; state variables are Reserves(E), Structure (V) and Maturity & reproduction (E_R), in white boxes. Dark arrows are energy fluxes and dotted ones show temperature influence on these rates.

FIGURE 2. Graphical representation of the preferential interaction between substrates in the Synthetizing Unit concept (Kooijman, 2010), that allows the substitution of one substrate type to another. S_X is the substrate corresponding to the microalgal cells and S_Y the one for remaining POM. θ. represents a free SU fraction while θ_X and θ_Y are SU fractions bound respectively to a X-type food particle and a Y-type food particle. P stands for the product released after transformation of the substrate.

FIGURE 3. Map of the Bay of Brest with the location of the sampling area for monthly monitoring of great scallops (indicated in gray), named Roscanvel and the two environmental monitoring sites: the REPHY station at Lanvéoc and the SOMLIT station at Sainte-Anne.

FIGURE 4. Environmental forcing variables monitored in the Bay of Brest between 1998 and 2003. Sea bottom temperature were measured on the Roscanvel bank (doted line, in Celcius degrees). Phytoplankton enumeration (dark line, in cells per liter) come from the REPHY monitoring station (PHYtoplankton and PHYcotoxins monitoring NEtwork, Ifremer) in Lanvéoc. Particulate Organic Matter to which cells counting have been deducted (gray line, in particles per liter) were measured by the SOMLIT monitoring station in Sainte-Anne (data provided by "Service d'Observation en Milieu Littoral, INSU-CNRS, Brest").

FIGURE 5. Simulation of *P. maximus* shell length over a full life-cycle using the primary parameters of the DEB model (dark line). Dots are a collection of shell length data collected over decades in the bay of Brest and archived in the EVECOS time series (EVECOS data base provided by "Observatoire Marin de l'IUEM, INSU, Plouzané").

FIGURE 6. Scaled functional responses for the different food proxies in simulations of three-year-old *P. maximus* in the Bay of Brest between 1998 and 2003. The doted curve represents the scaled functional response f_Y for POM food

25

type, the gray line is for scaled functional response f_X for the microalgae food type and the resulting total scaled functional response f is plotted by the dark line.

FIGURE 7. Simulated flesh dry weight (in g) of an average three-year-old individual of *P. maximus* in the Bay of Brest between 1998 and 2003, using phytoplankton counting (continuous dark line) and using POM as a supplementary food source (dotted dark line). Dots are observed mean flesh dry weights (average on 20 individuals) of three-year-old great scallops collected in the Bay of Brest between 1998 and 2003 (EVECOS data base provided by "Observatoire Marin de l'IUEM, INSU, Plouzané"). Gray curves are upper and lower limits of the confidence interval (p = 0.05) for measurements.

FIGURE 8. Simulated (dark line) daily shell growth rate (DSGR, in $\mu m.d^{-1}$) of an average three-year-old individual of *P. maximus* and mean DSGR (gray line) calculated on ten individuals of three-year-old great scallops collected in the Bay of Brest between 1998 and 2003 (EVECOS data base provided by "Observatoire Marin de l'IUEM, INSU, Plouzané").

FIGURE 9. Simulated shell length (in cm) of an average three-year-old individual of *P. maximus* in the Bay of Brest between 1998 and 2003, using phytoplankton counting (continuous dark line) and using POM as a supplementary food source (dotted dark line). Gray line is the observed mean shell length, measured on ten individuals of three-year-old great scallops collected in the Bay of Brest between 1998 and 2003 (EVECOS data base provided by "Observatoire Marin de l'IUEM, INSU, Plouzané").

FIGURE 10. Simulated gonado-somatic index (GSI, in g) of an average three-year-old individual of *P. maximus* in the Bay of Brest between 1998 and 2003, using phytoplankton counting (continuous dark line) and using POM as a supplementary food source (dotted dark line). Dots are observed mean GSI (average on 20 individuals) of three-year-old great scallops collected in the Bay of Brest between 1998 and 2003 (EVECOS data base provided by "Observatoire Marin de l'IUEM, INSU, Plouzané"). Gray curves are upper and lower limits of the confidence interval (p = 0.05) for measurements.

FIGURE 11. Simulated growth of an average individual of *P. maximus* in the Bay of Brest, from its birth in June 1998 until 2003. Shell length (dark line, in cm) is compared to the collection of shell length data (dots), gathered over decades in the Bay of Brest and archived in the EVECOS time series (EVECOS data base provided by "Observatoire

Marin de l'IUEM, INSU, Plouzané"). Daily shell growth rate (in $\mu m.d^{-1}$) is the gray line. Environmental variables (temperature and food markers) are the same as those used in simulations of three-year-old scallops.

FIGURE 12. Simulated (dark line) daily shell growth rate (DSGR, in $\mu m.d^{-1}$) of an average three-year-old individual of *P. maximus* and observed mean DSGR (gray line), calculated on ten individuals of three-year-old great scallops collected in the Bay of Brest (EVECOS data base provided by "Observatoire Marin de l'IUEM, INSU, Plouzané") in 1999 (A) and 2001 (B). Sea bottom temperature (gray doted line, in Celsius degrees) and the total functional response f (dark dotted line) are also plotted.

Figures

FIGURE 1: Conceptual scheme of the DEB model applied to the scallop *P. maximus*. Forcing variables (food and temperature) are in gray ; state variables are Reserves(E), Structure (V) and Maturity & reproduction (E_R), in white boxes. Dark arrows are energy fluxes and dotted ones show temperature influence on these rates.
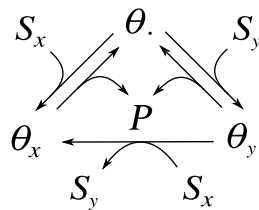
FIGURE 2: Graphical representation of the preferential interaction between substrates in the Synthetizing Unit concept (Kooijman, 2010), that allows the substitution of one substrate type to another. S_X is the substrate corresponding to the microalgal cells and S_Y the one for remaining POM. $\theta.$ represents a free SU fraction while θ_X and θ_Y are SU fractions bound respectively to a X-type food particle and a Y-type food particle. P stands for the product released after transformation of the substrate.

FIGURE 3: Map of the Bay of Brest with the location of the sampling area for monthly monitoring of great scallops (indicated in gray), named Roscanvel and the two environmental monitoring sites: the REPHY station at Lanvéoc and the SOMLIT station at Sainte-Anne.

FIGURE 4: Environmental forcing variables monitored in the Bay of Brest between 1998 and 2003. Sea bottom temperature were measured on the Roscanvel bank (doted line, in Celcius degrees). Phytoplankton enumeration (dark line, in cells per liter) come from the REPHY monitoring station (PHYtoplankton and PHYcotoxins monitoring NEtwork, Ifremer) in Lanvéoc. Particulate Organic Matter to which cells counting have been deducted (gray line, in particles per liter) were measured by the SOMLIT monitoring station in Sainte-Anne (data provided by "Service d'Observation en Milieu Littoral, INSU-CNRS, Brest").

FIGURE 5: Simulation of *P. maximus* shell length over a full life-cycle using the primary parameters of the DEB model (dark line). Dots are a collection of shell length data collected over decades in the bay of Brest and archived in the EVECOS time series (EVECOS data base provided by "Observatoire Marin de l'IUEM, INSU, Plouzané").

FIGURE 6: Scaled functional responses for the different food proxies in simulations of three-year-old *P. maximus* in the Bay of Brest between 1998 and 2003. The doted curve represents the scaled functional response f_Y for POM food type, the gray line is for scaled functional response f_X for the microalgae food type and the resulting total scaled functional response f is plotted by the dark line.

FIGURE 7: Simulated flesh dry weight (in g) of an average three-year-old individual of *P. maximus* in the Bay of Brest between 1998 and 2003, using phytoplankton counting (continuous dark line) and using POM as a supplementary food source (dotted dark line). Dots are observed mean flesh dry weights (average on 20 individuals) of three-year-old great scallops collected in the Bay of Brest between 1998 and 2003 (EVECOS data base provided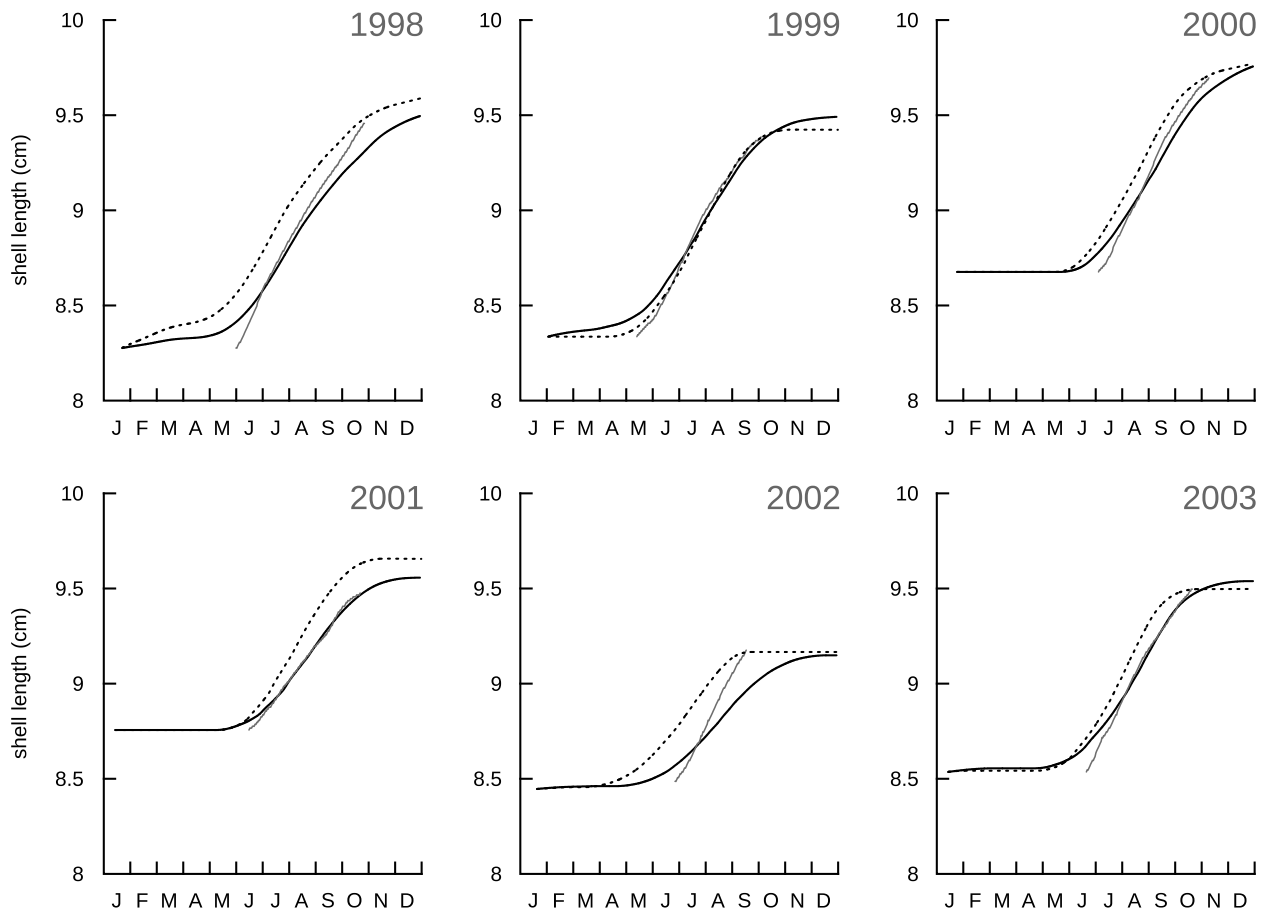 by "Observatoire Marin de l'IUEM, INSU, Plouzané"). Gray curves are upper and lower limits of the confidence interval (p = 0.05) for measurements.

FIGURE 8: Simulated (dark line) daily shell growth rate (DSGR, in $\mu m.d^{-1}$) of an average three-year-old individual of *P. maximus* and mean DSGR (gray line) calculated on ten individuals of three-year-old great scallops collected in the Bay of Brest between 1998 and 2003 (EVECOS data base provided by "Observatoire Marin de l'IUEM, INSU, Plouzané").

FIGURE 9: Simulated shell length (in cm) of an average three-year-old individual of *P. maximus* in the Bay of Brest between 1998 and 2003, using phytoplankton counting (continuous dark line) and using POM as a supplementary food source (dotted dark line). Gray line is the observed mean shell length, measured on ten individuals of three-year-old great scallops collected in the Bay of Brest between 1998 and 2003 (EVECOS data base provided by "Observatoire Marin de l'IUEM, INSU, Plouzané").
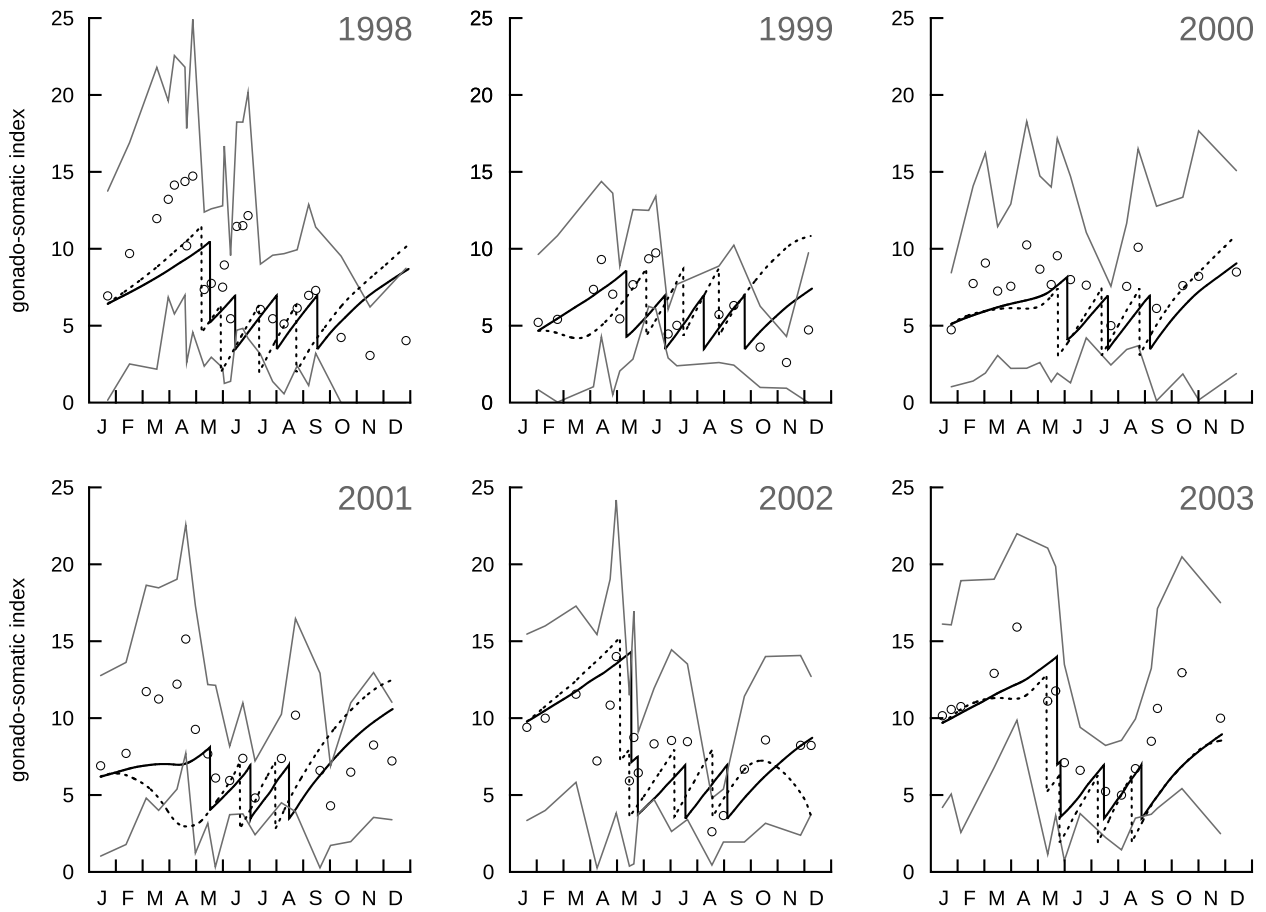
FIGURE 10: Simulated gonado-somatic index (GSI, in g) of an average three-year-old individual of *P. maximus* in the Bay of Brest between 1998 and 2003, using phytoplankton counting (continuous dark line) and using POM as a supplementary food source (dotted dark line). Dots are observed mean GSI (average on 20 individuals) of three-year-old great scallops collected in the Bay of Brest between 1998 and 2003 (EVECOS data base provided by "Observatoire Marin de l'IUEM, INSU, Plouzané"). Gray curves are upper and lower limits of the confidence interval (p = 0.05) for measurements.
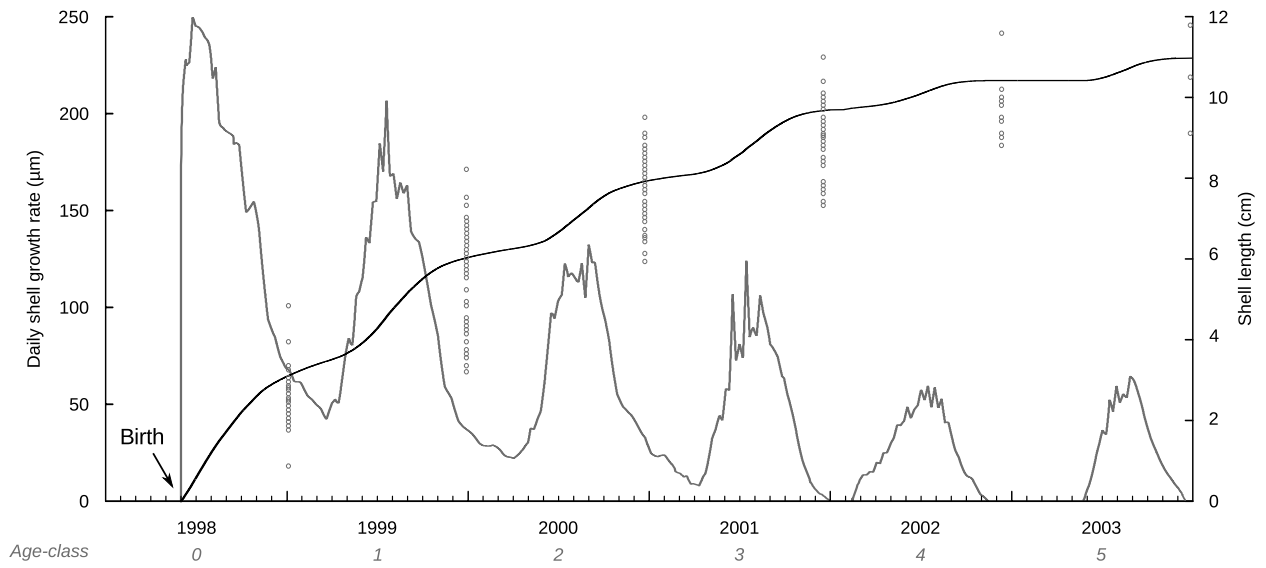
FIGURE 11: Simulated growth of an average individual of *P. maximus* in the Bay of Brest, from its birth in June 1998 until 2003. Shell length (dark line, in cm) is compared to the collection of shell length data (dots), gathered over decades in the Bay of Brest and archived in the EVECOS time series (EVECOS data base provided by "Observatoire Marin de l'IUEM, INSU, Plouzané"). Daily shell growth rate (in μm.d^{-1}) is the gray line. Environmental variables (temperature and food markers) are the same as those used in simulations of three-year-old scallops.
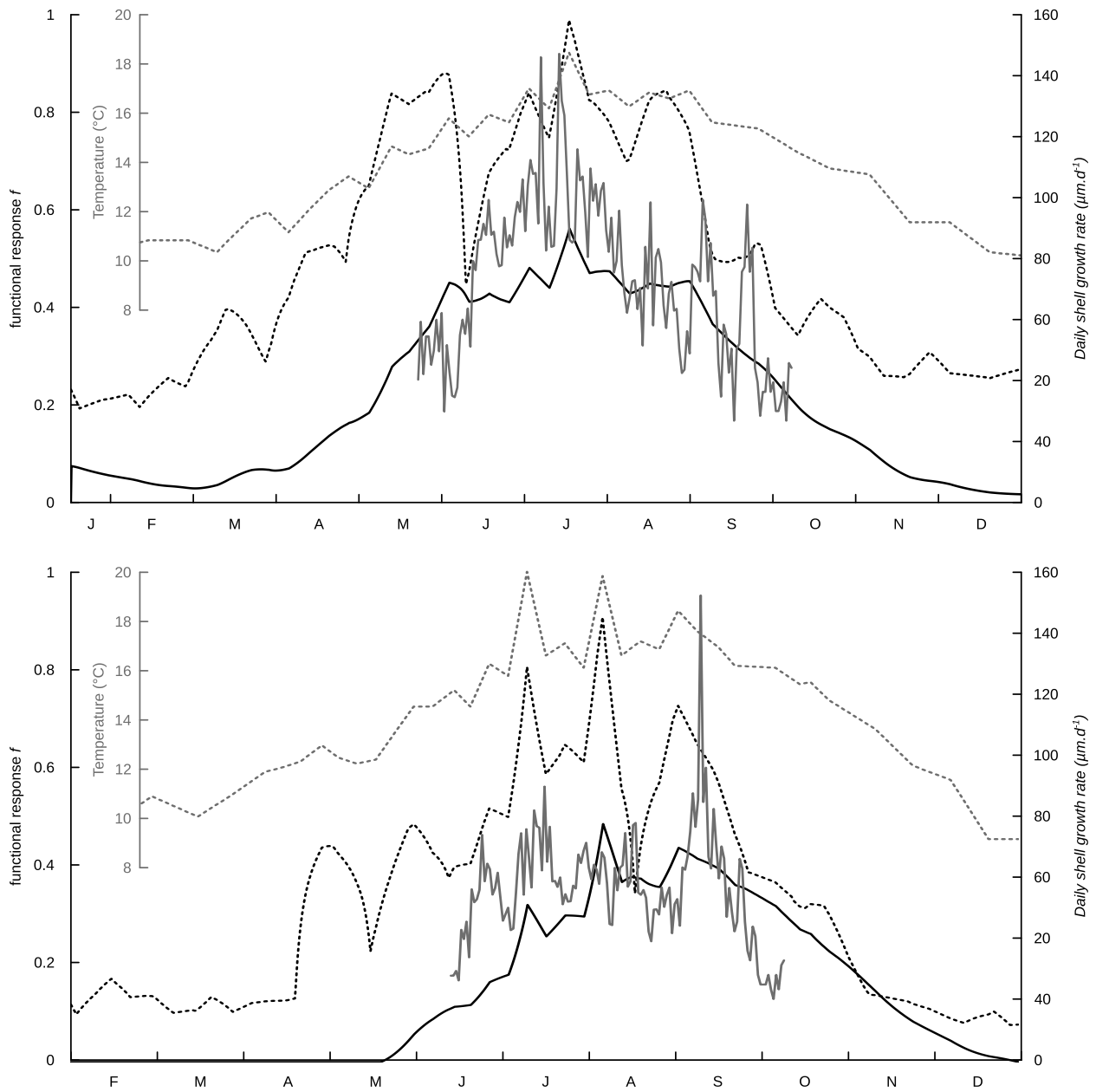
FIGURE 12: Simulated (dark line) daily shell growth rate (DSGR, in μm.d^{-1}) of an average three-year-old individual of *P. maximus* and observed mean DSGR (gray line), calculated on ten individuals of three-year-old great scallops collected in the Bay of Brest (EVECOS data base provided by "Observatoire Marin de l'IUEM, INSU, Plouzané") in 1999 (A) and 2001 (B). Sea bottom temperature (gray doted line, in Celsius degrees) and the total functional response f (dark dotted line) are also plotted.